Convex-hull mass estimates of the dodo (*Raphus cucullatus)*: application of a CT-based mass estimation technique

Charlotte A Brassey, Thomas G O'Mahoney, Andrew C Kitchener, Phillip L Manning, William I Sellers

The external appearance of the dodo (*Raphus cucullatus*) has been a source of considerable intrigue as contemporaneous accounts or depictions are rare. The body mass of the dodo has been particularly contentious, with the flightless pigeon alternatively reconstructed as slim or overweight depending upon the skeletal metric used as the basis for mass prediction. Resolving this dichotomy and obtaining a reliable estimate for mass is essential before future analyses regarding dodo life history, physiology or biomechanics can be conducted. Previous mass estimates of the dodo have relied upon predictive equations based upon hind limb dimensions of extant pigeons. Yet the hind limb proportions of dodo have been found to differ considerably from those of their modern relatives, particularly with regards to midshaft diameter. Therefore, application of predictive equations to unusually robust fossil skeletal elements may bias mass estimates. We present a whole-body computed tomography (CT) -based mass estimation technique for application to the dodo. We generate 3D volumetric renders of the articulated skeletons of 20 species of extant pigeons, and wrap minimum-fit 'convex hulls' around their bony extremities. Convex hull volume is subsequently regressed against mass to generate predictive models based upon whole skeletons. Our best-performing predictive model is characterized by high correlation coefficients and low mean squared error (a=-2.31, b=0.90, r^2=0.97, MSE=0.0046). When applied to articulated composite skeletons of the dodo (National Museums Scotland, NMS.Z.1993.13; Natural History Museum, NHM A.9040 and S/1988.50.1), we estimate eviscerated body masses of 8-10.8 kg. When accounting for missing soft tissues, this may equate to live masses of 10.6-14.3 kg. Mass predictions presented here fall towards the lower end of those previously published, and support recent suggestions of a relatively slim dodo. CT-based reconstructions provide a means of objectively estimating mass and body segment properties of extinct species using whole articulated skeletons.

Convex-hull mass estimates of the dodo (*Raphus cucullatus)*: application of a CT-based mass estimation technique

Brassey, C.A.[1]*, O'Mahoney, T.[1], Kitchener, A.C.[2,3], Manning, P. L.[4], Sellers, W.I.[1]

[1]Faculty of Life Sciences, University of Manchester, Manchester M13 9PL

[2]Department of Natural Sciences, National Museums Scotland, Edinburgh EH1 1JF

[3] Institute of Geography, School of Geosciences, University of Edinburgh, Drummond Street, Edinburgh, EH8 9XP

[4]Interdisciplinary Centre for Ancient Life, School of Earth, Atmospheric and Environmental Sciences, University of Manchester, Manchester M13 9PL

*corresponding author (charlotte.brassey@manchester.ac.uk)

Abstract

The external appearance of the dodo (*Raphus cucullatus,* Linnaeus, 1758) has been a source of considerable intrigue as contemporaneous accounts or depictions are rare. The body mass of the dodo has been particularly contentious, with the flightless pigeon alternatively reconstructed as slim or fat depending upon the skeletal metric used as the basis for mass prediction. Resolving this dichotomy and obtaining a reliable estimate for mass is essential before future analyses regarding dodo life history, physiology or biomechanics can be conducted.

Previous mass estimates of the dodo have relied upon predictive equations based upon hind limb dimensions of extant pigeons. Yet the hind limb proportions of dodo have been found to differ considerably from those of their modern relatives, particularly with regards to midshaft diameter. Therefore, application of predictive equations to unusually robust fossil skeletal elements may bias mass estimates. We present a whole-body computed tomography (CT) -based mass estimation technique for application to the dodo. We generate 3D volumetric renders of the articulated skeletons of 20 species of extant pigeons, and wrap minimum-fit 'convex hulls' around their bony extremities. Convex hull volume is subsequently regressed against mass to generate predictive models based upon whole skeletons.

Our best-performing predictive model is characterized by high correlation coefficients and low mean squared error (a=-2.31, b=0.90, r^2=0.97, MSE=0.0046). When applied to articulated composite skeletons of the dodo (National Museums Scotland,

NMS.Z.1993.13; Natural History Museum, NHMUK A.9040 and S/1988.50.1), we estimate eviscerated body masses of 8-10.8 kg. When accounting for missing soft tissues, this may equate to live masses of 10.6-14.3 kg. Mass predictions presented here fall towards the lower end of those previously published, and support recent suggestions of a relatively slim dodo. CT-based reconstructions provide a means of objectively estimating mass and body segment properties of extinct species using whole articulated skeletons.

Introduction

Body mass (M_b) is a fundamental descriptor of an organism and co-varies with important ecological and physiological traits, such as population density, metabolism and cost-of-transport [1]. Key evolutionary scenarios, such as the origin of avian flight [2] and the extinction of island flightless avian species [3], have been diagnosed on the basis of estimated M_b. Therefore, the reconstruction of body mass in extinct bird species is a subject of considerable interest within the palaeontological and evolutionary biology literature [2–6].

An often-applied technique for estimating the body mass of an extinct vertebrate has been to measure a skeletal dimension from modern species, such as femur circumference [7] or glenoid diameter [8], and apply this as the independent variable in a regression against body mass. However, 'overdevelopment' of the pelvic apparatus has been found to be significantly correlated with the flightless condition in extant birds [9]. Therefore, the application of mass prediction equations, based solely on hind limb material of flightless avian taxa, has been questioned in extinct species such as the moa [6].

The dodo (*Raphus cucullatus*, Linnaeus, 1758 [10]) is an iconic representative of island flightlessness and human-induced extinction, and its external appearance has been a source of considerable intrigue due to the scarcity of contemporaneous accounts or depictions [11]. This extinct flightless columbiform was endemic to the island of Mauritius. However, the skeletal anatomy of the dodo is comparatively well known, and

its pelvic morphology has been thoroughly investigated. Hind limb bones of *R. cucullatus* have been found to differ considerably in both their length and width relative to their volant relatives [11, although see 12]. Yet previous attempts to estimate the body mass of the dodo have predominantly relied upon predictive equations derived solely from the hind limb metrics of extant species [14–16].

An alternative approach to mass estimation involves the reconstruction of 3D volumetric models. An early volumetric reconstruction of the dodo was conducted by physically sculpting a scale model of an individual and estimating volume via fluid displacement [13]. Whilst such volumetric techniques are less liable to bias by individual robust/gracile postcranial elements than traditional linear bivariate equations, they do inevitably involve some degree of artistic licence in the sculpting of soft tissue contours and require an estimate for fossil body density to be assigned.

Following advances in 3D imaging technology, the use of digital skeletal models in mass estimation of fossil skeletons has become increasingly popular [17–20]. These studies typically involve the ‘wrapping’ of geometric shapes or lofted smooth surfaces around the skeleton in order to replicate the original soft tissue contour of the animal. Zero-density cavities such as lung and tracheal space may also be modeled [21]. However, similar to physical sculpting with clay, assumptions must still be made regarding body density and the extent of soft tissues beyond the skeleton. Therefore, it is essential that reconstructions are grounded within a quantitative understanding of extant species in order to avoid subjective modeling of soft tissues (both body and plumage).

Here we present new mass estimates for the dodo based on an alternative 'convex hull' volumetric reconstruction approach [22,23]. The convex hull (*CH*) of a set of points is defined as the smallest convex polytope that contains all said points, and intuitively can be thought of as a shrink-wrap fit around an object (see Figure 1). Application of the convex hulling technique to mass estimation does not involve any subjective reconstruction of soft tissue anatomy and solely relies upon the underlying skeleton. We calculate minimum convex hull volumes for a sample of composite articulated dodo skeletons, and convert these to body mass estimates using a computed tomography (CT) calibration dataset of 20 species of extant pigeon. To our knowledge, this is the first time such an extensive CT dataset of extant animals has been used to reconstruct the body mass of a fossil of an extinct species.

Methods and Materials

The modern dataset consists of 20 columbiform individuals, spanning a wide variety of body sizes from a 70 g fruit dove (*Ptilinopus;* Swainson, 1825 [24]) up to the largest extant pigeon, the 2 kg Victoria crowned pigeon (*Goura victoria*; Fraser, 1844 [25]). We also cover a broad taxonomic range (including the closest extant relative of the dodo [26], the Nicobar pigeon (*Caloenas nicobarica*; Linnaeus, 1758 [10]*)*). Frozen carcasses were sourced from National Museums Scotland, Edinburgh, and the University of Manchester (see Table 1). Carcasses were CT scanned at Leahurst Veterinary School, University of Liverpool, in a Toshiba Aquilion PRIME helical scanner at a slice thickness of 0.5mm and a pixel spacing of between 0.24-0.51mm, depending on the maximum size of the specimen. 3D models of the skeletons were generated in Seg3D [27], using an automatic threshold with subsequent manual masking to remove the dense rachises attached to the forelimb.

Models were exported into Geomagic Studio (www.geomagic.com), where each skeleton was divided into functional units (skull, neck, trunk, humerus, radius+ulna, carpometacarpals, femur, tibiotarsus+fibula, tarsometatarsus, feet). The cervical series was further subdivided in order to achieve a tight-fitting hull around the curving neck. Minimum convex hulls were calculated in MATLAB (www.mathworks.com), using the 'convhull' function implementing the Quickhull (qhull) algorithm [28], and total convex hull volume was calculated as the sum of individual segment volumes (see Figure 1). Body mass was measured for each carcass, and the relationship between M_b and

convex hull volume (CH_{vol}) was estimated using ordinary least squares (OLS) regression on $\log_{10}$ transformed data. As the purpose of the regression was to derive a predictive equation, a type-I regression, such as OLS, was deemed most appropriate [29]. Additionally we accounted for the statistical non-independence of phylogenetically-related data points by carrying out phylogenetic generalized least squares (PGLS) regressions, implemented in MATLAB using 'Regression2' software [30]. A majority-rule consensus tree was calculated using the R package 'ape' [31] based upon a sample of 10,000 trees sourced from the birdtrees.org website [32] using the Hackett et al. [33] phylogeny as a backbone. All branch lengths were set to 1.

To reconstruct the body masses of articulated dodo skeletons, we generated 3D digital models of these specimens. The Edinburgh dodo (National Museums Scotland, NMS.Z.1993.13) was scanned using a Z+F Imager 5010 LiDAR (Light Detection And Range) scanner and reconstructed in the Z+F LaserControl software. The Natural History Museum (NHMUK), London specimens (Tring skeleton, S/1988.50.1; South Kensington specimen NHM A9040) were digitized using the photogrammetric technique detailed elsewhere [34,35] and reconstructed in VisualSFM [36]. Despite application of two alternative imaging techniques, previous studies have found the results obtained via photogrammetry and laser scanning to be comparable [34], and convex hull results to be insensitive to point cloud density [23,37]. 3D models of the dodo skeletons were cleaned up in Geomagic and subdivided into functional units. Our only intervention with the dodo models was to mirror the right hand side of the Edinburgh ribcage to account for missing ribs on its left side. Convex hulls were fitted according to the methodology

146 applied to modern pigeons.

147 The largest extant pigeon (*G. victoria*) weighs on average 2.3 kg [38], a value far below
148 all previous estimates of dodo mass. When applying a pigeon-based equation to predict
149 dodo body mass, it is therefore necessary to extrapolate beyond the body size range
150 upon which the predictive model is based. By restricting ourselves to phylogenetically
151 closely related species, the fossil species of interest may therefore be up to an order of
152 magnitude greater in size than any extant relative. Furthermore the majority of modern
153 pigeons included in this dataset are proficient fliers and have likely been subject to very
154 different evolutionary pressures than the flightless dodo.

155 For this reason, we also applied a previously published convex hull equation derived
156 from extant ratites and galloanserae birds, extending the range of body masses beyond
157 60 kg and incorporating ground-dwelling species. Raw data are taken from Brassey et
158 al [23], whilst the axes have been inverted ($\log_{10}$ volume as the independent variable vs.
159 $\log_{10}$ mass as the dependent variable) to create a predictive model. Standard OLS
160 regression was preferred as previous analyses found uncorrected type-I models to fit
161 the data better than phylogenetically corrected regressions [23]. It must be emphasized
162 that the non-pigeon data are derived from an earlier study applying a different imaging
163 technique (light detection and range, LiDAR, on museum mounted skeletons) and uses
164 literature-assigned values for mass due to lack of associated body masses. Whilst the
165 previous study found no significant impact on calculated CH_{vol} due to variation in point
166 cloud density associated with different imaging techniques, caution should be exercised
167 when comparing the regression models.

168 **Results**

169 Total convex hull volumes for the modern pigeons are reported in Table 1, and
170 segment-specific CH_{vol} values can be found in Supplementary Material S1. Convex hull
171 models are available for download from http://www.animalsimulation.org. We found
172 considerable variation between frozen pigeon specimens in the posture of the digits
173 forming the foot i.e. adduction vs. abduction of the digits. This influenced the overall
174 shape, and hence calculated CH_{vol}, of the foot functional units (see Figure 1D). Given
175 repositioning of the skeleton was not possible due to the frozen nature of the carcasses,
176 here we report total CH_{vol} values with and without feet included. External inspection of
177 the carcasses suggested evisceration had been carried out on some specimens. Using
178 CT scans the occurrence of evisceration was confirmed across our modern dataset (see
179 Table 1). Therefore, we report separate predictive models derived from 'eviscerated'
180 carcasses (n=13), 'intact' carcasses (n=7), and a third 'combined' model comprising
181 both eviscerated and intact specimens (n=20).
182
183 The results of the OLS regression analyses are presented in Table 2, and
184 phylogenetically corrected (PGLS) regressions are given in Supplementary Material S2
185 alongside the composite phylogeny used in this analysis. PGLS regressions did not
186 provide a better fit to the data than uncorrected OLS regressions (as determined by
187 Akaike Information Criterion values, AIC) for the 'eviscerated' and 'combined' models
188 (Table 2). However, a PGLS model was found to fit the 'intact' extant pigeon data better
189 than an uncorrected OLS model (Table 2).
190

191 Removing CH_{vol} of the feet from the analyses had very little effect on the results of the
192 regression, although mean squared error (MSE) decreased slightly in all models and
193 therefore only regression models minus feet are discussed any further in the text. Figure
194 2 illustrates a strong positive correlation between $M_{b\ and}$ CH_{vol} for the eviscerated
195 specimens within the sample (a=-2.31, b=0.90, r^2=0.97). In contrast, the relationship
196 between $M_{b\ and}$ CH_{vol} in intact specimens illustrates a weak positive correlation
197 characterized by low correlation coefficients and high mean square error (a=-1.06,
198 b=0.66, r^2=0.70). Intact specimens do not plot consistently above the eviscerated
199 pigeon slope (Figure 2) and are instead characterized by a high degree of scatter.
200 When combining the eviscerated and intact specimens into one dataset, M_b and CH_{vol}
201 remain tightly correlated (a=-2.08, b=0.85, r^2=0.92).
202
203 Total CH_{vol} calculated for the mounted dodo skeletons are reported in Table 3 (see
204 Supplementary Material S3 for segment-specific values) and an example of a
205 photogrammetric model is illustrated in Figure 3. Using the 'eviscerated' predictive
206 model, dressed M_b is estimated as 8.0 kg (95% prediction interval (PI) 4.6-13.9 kg), 8.7
207 kg (95%PI 5.0-15.0 kg) and 10.8 kg (95%PI 6.1-19.0 kg) respectively for the NHMUK
208 Tring, NHMUK South Kensington and Edinburgh dodos. Applying the 'combined'
209 predictive equation results in wider and therefore more conservative prediction intervals
210 (NHMUK Tring, 6.7 kg 95%PI 3.5-13.1 kg; NHMUK South Kensington, 7.3 kg 95%PI
211 3.7-14.3 kg; Edinburgh, 9.0 kg 95%PI 4.5-17.9 kg).
212

213 The results of the OLS regression of convex hull volume against body mass for a
214 dataset of ground-dwelling ratites and galloanserae derived from Brassey et al [23] are
215 presented in Table 2. This relationship is also characterized by high correlation
216 coefficients (a=-1.65, b=0.82, r^2=0.97), and results in *intact* mass estimates of 10.9 kg
217 (95%PI 5.7-20.6 kg), 11.6 kg (95%PI 6.1-22.1 kg) and 14.0 kg (95%PI 7.3-26.6 kg)
218 respectively for the NHMUK Tring, NHMUK South Kensington and Edinburgh dodos.
219
220 Figure 4 illustrates the distribution of segment-specific convex hull volumes as a
221 proportion of total CH_{vol} within the models. In extant pigeons trunk CH_{vol} represents on
222 average 69% of total CH_{vol}. The NHMUK Tring dodo skeleton has a percentage trunk
223 volume significantly lower than that of extant pigeons (67%, 1-tailed t-test, t=3.23,
224 p<0.01), whilst percentage trunk volume in the NHMUK South Kensington and
225 Edinburgh skeletons is significantly higher than extant pigeons (71% and 80%, t=-2.23
226 and -13.0 respectively, p<0.05). With the exception of the tarsometatarsii of the NHMUK
227 South Kensington skeleton, pelvic convex hull segments of the dodos comprise a
228 significantly greater proportion of total CH_{vol} than in extant pigeons (p<0.05). In contrast,
229 dodo pectoral convex hull segments contribute proportionally less to total CH_{vol} than in
230 extant pigeons (p<0.0001) (Figure 4).

Discussion

Predictive equation derived from modern CT dataset

To our knowledge the present study represents the first application of a predictive equation derived solely from whole-body CT to the problem of body mass estimation for extinct animals. Previous volumetric mass estimate studies have relied upon articulated skeletons of extant species to derive a calibration equation [6,22]. Yet articulated skeletons are often missing crucial specimen information, such as a recorded body mass. By working with frozen carcasses, body mass is directly measurable and uncertainties associated with mounting and posing of the skeletons can be avoided [23].

Our dataset consists of both 'intact' and 'eviscerated' pigeons as determined by examination of CT scans. Previous analyses of carcass composition have found eviscerated mass to represent 62-66% of live body mass in rock doves [39,40], yet no data exist regarding the possible scaling of internal organ mass across a range of body sizes in the Columbiformes. As can be seen in Figure 2, there is no consistent disparity between intact and eviscerated specimens, and the relationship between M_b and CH_{vol} in intact pigeons is relatively weak (r^2=70, p=0.019). This correlation improves considerably when accounting for phylogeny (Supplementary Material S2), but remains weaker than the relationship between M_b and CH_{vol} characterizing eviscerated specimens. Live body mass has been shown to vary considerably in wild animals due to hydration, nutrition and gut content [41] and therefore some degree of scatter is to be expected in intact carcasses. Particularly striking is the variability in gizzard contents between similar-sized specimens visible in CT scans (see Figure 5).

254

255 This suggests intact pigeon M_b cannot be corrected for the presence of internal organs
256 using a single factor representing average percentage eviscerated mass as a function
257 of live mass (i.e. multiplying by values of 0.62 or 0.66 previously found in the literature).
258 Additionally, attempting to correct intact M_b by substituting intact CH_{vol} into the
259 eviscerated regression model would be highly circular and result in artificially inflated
260 correlation coefficients, if the equation were used in a predictive capacity. Therefore, we
261 apply both the uncorrected OLS eviscerated model and combined (eviscerated and
262 intact) model to bracket the range of likely dodo body masses. Interestingly, the very
263 high correlation coefficient and low mean squared error of the eviscerated equation
264 suggest that once the variability associated with fluid and gut content is removed, the
265 relationship between the mass of the remaining musculoskeletal system and CH_{vol} is
266 more tightly constrained.

267

268 ***Volumetric body mass estimation applied to the dodo***

269 No reliable records of the body mass of dodo exist prior to its extinction in the 17th
270 Century and subsequent mass estimates have varied considerably. Early accounts of
271 the flightless bird suggested an average mass of 50 lb (22 kg) [42], although such
272 accounts “have a tendency towards exaggeration” [11]. More recently a ‘slim’ dodo
273 (mean 10.2 kg) was proposed on the basis of femoral, tibiotarsal and tarsometatarsal
274 length scaling in modern birds [14]. However hind limb bone length has been shown to
275 correlate poorly with body mass relative to other cross-sectional geometric properties
276 and frequently contains a strong functional signal [8,43–45]. Alternatively, a predictive

277 equation based on femoral and tibiotarsal least circumference in ground-dwelling birds
278 has suggested mass estimates between 9.5-12.3 kg [15].
279
280 The application of volumetric mass estimation techniques to the dodo has been rare. A
281 sculpted scale model of a ‘slim’ dodo based upon mean skeletal measures was created
282 to replicate sketches dating contemporaneously to its survival on Mauritius and resulted
283 in mass estimated of 12.5-16.1 kg [13]. In the same study a ‘fat’ dodo model based on
284 later ‘exaggerated’ artworks was predicted to weigh between 21.7-27.8 kg.
285
286 Here we estimate mean eviscerated body masses for articulated composite dodo
287 skeletons of between 8.0-10.8 kg. Without further information regarding the effect of
288 within-subject variability in gizzard, crop or gut content or interspecific scaling of viscera
289 mass, any extrapolation to a live mass should be treated with caution. However, with
290 this caveat in mind, a 33% increase in mass to account for missing organs (as
291 quantified in extant *C. livia*) would take our results to 10.6-14.3 kg. This overlaps with
292 the slim sculpted model based on contemporaneous accounts [13]. Including our 95%
293 prediction intervals takes both the NHMUK Tring and South Kensington skeletons to a
294 maximum of 18.2 kg and 19.9 kg whole body masses, still considerably below the 22kg
295 suggested historically [42]. In contrast, the 95% prediction intervals of the Edinburgh
296 dodo include 22kg once multiplied by 1.33.
297
298 Unlike all previous volumetric studies, our convex hulling technique does not require a
299 value for body density to be assigned from the literature. Instead we directly derive the

300 relationship between M_b and CH_{vol} in order to avoid uncertainty regarding assigning
301 literature values, which have been shown to differ considerably across avian groups and
302 with various methodologies for estimating body density [17]. However, this does
303 implicitly rely upon the predictive equation being applied to a fossil of an extinct species
304 that is closely related to (and can therefore be assumed to share a similar body density
305 to) the modern dataset from which the predictive equation was derived. In this case of
306 estimating dodo mass based on extant pigeons, we believe this assumption can be
307 upheld. Alternatively, CH_{vol} may be multiplied by a given value of carcass density to give
308 a hard lower limit to body mass (as carcass volume cannot be less than convex hull
309 volume). The sole literature value for intact feathered pigeon density is 648kg/m^3 from
310 Hamershock et al. [46], producing hard lower bounds to estimated body mass 5.8kg,
311 6.3kg, and 7.9kg for the Tring, Kensington and Edinburgh composite skeletons
312 respectively.
313
314 Previous authors have cautioned over the extrapolation of regression models beyond
315 the limits of the extant dataset when applied in a predictive capacity [47]. To avoid this
316 scenario, here we also apply a convex hull predictive model previously derived from
317 ratites and ground-dwelling galloanserae birds [23] to the mounted dodo specimens.
318 This results in mass estimates for the *intact* dodo ranging between 10.8-14.0 kg,
319 remarkably similar to those values tentatively reconstructed by correcting the
320 eviscerated pigeon model for missing viscera content. This further strengthens the
321 argument for the reconstruction of a relatively slim dodo, and suggests extrapolation of

the predictive equation beyond the range of modern pigeons does not, *in this instance,* result in implausible mass estimates.

We consider the convex hulling technique to be superior to other sculpting-based volumetric methods (such as manual sculpting with clay [13] or digital sculpting with non-uniform rational B-spline (NURBs) curves [20]) for the purpose of mass estimation as soft tissues and hypothesized respiratory systems need not be reconstructed for fossils of extinct species, and the technique is entirely repeatable. When values for centre of mass (COM) and segment inertial properties are required for further biomechanical analyses, NURBs may be required in order to achieve a representative mass distribution across the skeleton. In such situations it is essential that soft tissue reconstructions are based on quantitative comparative dissection data from relevant modern species in order to minimize subjectivity in model creation. However, for the sole purpose of mass estimation, convex hulling should be the preferred technique.

Composite and articulated skeletons

The dodo specimens included in this study are composite skeletons, comprising skeletal material from more than one individual and including sculpted or cast elements. Therefore, our study is limited to estimating the body mass of the hypothetical animal represented by each articulated skeleton, rather than a known individual. Currently there exists only one near-complete dodo skeleton comprising a single individual (the Thirioux dodo), upon which research is currently still continuing [48].

345 Whilst the use of composite skeletons should clearly be treated with caution when used
346 in biomechanical analyses, their composite nature does not entirely rule out their use,
347 particularly in the case of mass estimation. A recent large-scale macroevolutionary [49]
348 study of body size in a fossil lineage relied upon mass data derived solely from humeral
349 and femoral circumferences of one individual specimen per species. While this
350 approach is often the only one feasible, given the highly fragmentary nature of the fossil
351 record, taking one individual as being representative of an entire species leaves us
352 vulnerable to the possibility of high levels of intraspecific variation.
353
354 In contrast, a volumetric reconstruction based on a composite skeleton may be more
355 likely to reflect a species average by virtue of being a combination of several individuals
356 and could be less skewed by isolated robust or gracile elements. If subsequent
357 biomechanical analyses are to be carried out (such as finite element analysis on a
358 particular musculoskeletal unit), then it is important that the body mass entered into the
359 analyses is representative of that specific individual. However, for the case of volumetric
360 body mass estimation alone, it ought to be possible to derive a representative species
361 mean from a composite skeleton.
362
363 Of more concern is the frequency of missing, deformed or reconstructed material within
364 a fossil mount. Known issues with the dodo mounts included in this study include
365 missing ribs (Edinburgh skeleton), missing carpals (NHMUK South Kensington
366 skeleton), deformation of the fragile pubis (NHMUK South Kensington skeleton) or the
367 loss of the most of the ischium, pubis and caudal vertebrae (NHMUK Tring skeleton).

For a given object, the extent of the convex hull fitted to that object is dictated solely by its geometric extremes. In many ways this is advantageous for volumetric fossil reconstructions as damage occurring within the bounds of the convex hull does not affect our volume estimate. However when extremities are missing (such as the caudal tip of the pubis), the shape and volume of the convex hull are strongly affected. This is evident in the low percentage trunk volume of the NHMUK Tring skeleton (Figure 5) compared to those of extant pigeons and other dodos.

Whilst some evidence of underdevelopment of pectoral elements and overdevelopment of pelvic elements in the dodo is discernable relative to extant volant pigeons, Figure 5 predominantly illustrates the important contribution of trunk volume to total mass estimates. The Edinburgh skeleton has a proportionally more voluminous trunk than that of extant pigeons and other dodo skeletons, and therefore all other skeletal elements contribute proportionally less to total $CH_{vol.}$ The more voluminous trunk relative to other specimens may be attributed to the anterior positioning of the sternum due to constraints associated with the armature supporting the mount. The opposite is true of the NHMUK Tring skeleton, in which damage to the extremities of the pelvic girdle result in a reduced trunk volume. This highlights the sensitivity of volumetric reconstructions of fossils of extinct species to trunk morphology, and should be a concern when working with both composite and complete fossil specimens.

Summary

Here we present the first volumetric reconstruction of fossil body mass based entirely on modern whole-animal CT data. The eviscerated body mass of three articulated composite dodo skeletons is estimated to fall between 8.0-10.8 kg. When accounting for missing organ mass, our mean values still fall towards the lower range of previously published mass estimates. As the availability and cost of CT improves, we believe this non-subjective convex hull approach will become increasingly commonplace. Mass estimation of extinct species from fossils relies upon two key components; a reliable calibration equation derived from extant species, and an accurate reconstruction of the extinct individual from its fossil. We discuss the issues surrounding the use of articulated composite skeletons, and highlight the particular importance of trunk morphology to volume reconstructions. We suggest future efforts should focus on quantifying ribcage and sternal geometry in extant groups in order to bracket the possible trunk shape in fossils of extinct species.

Acknowledgements

We thank Zoller+Fröhlich (Z+F) Limited for their continued support, Jennifer Anné and Dr Victoria Egerton (University of Manchester), Martin Baker (University of Liverpool), Malgosia Nowak-Kemp (Oxford Museum of Natural History), Julian Hume, Judith White and Sandra Chapman (Natural History Museum, London), and the reviews of Heinrich Mallison and one anonymous referee.

References

1. Schmidt-Nielsen K. Scaling: Why is animal size so important? Cambridge: Cambridge University Press; 1984.

2. Turner AH, Pol D, Clarke JA, Erickson GM, Norell MA. A basal dromaeosaurid and size evolution preceding avian flight. Science (80-). 2007;317: 1378–1381. doi:10.1126/science.1144066

3. Boyer AG. Extinction patterns in the avifauna of the Hawaiian islands. Divers Distrib. 2008;14: 509–517. doi:10.1111/j.1472-4642.2007.00459.x

4. Hone DWE, Dyke GJ, Haden M, Benton MJ. Body size evolution in Mesozoic birds. J Evol Biol. 2008;21: 618–624. doi:10.1111/j.1420-9101.2007.01483.x

5. Butler RJ, Goswami A. Body size evolution in Mesozoic birds: Little evidence for Cope's rule. J Evol Biol. 2008;21: 1673–1682. doi:10.1111/j.1420-9101.2008.01594.x

6. Brassey CA, Holdaway RN, Packham AG, Anne J, Manning PL, Sellers WI. More Than One Way of Being a Moa: Differences in Leg Bone Robustness Map Divergent Evolutionary Trajectories in Dinornithidae and Emeidae (Dinornithiformes). PLoS One. 2013;8: e82668. doi:10.1371/journal.pone.0082668

7. Campione NE, Evans DC. A universal scaling relationship between body mass and proximal limb bone dimensions in quadrupedal terrestrial tetrapods. BMC Biol. 2012;10: 60.

8. Field DJ, Lynner C, Brown C, Darroch SAF. Skeletal Correlates for Body Mass Estimation in Modern and Fossil Flying Birds. PLoS One. 2013;8: e82000. doi:10.1371/journal.pone.0082000

9. Cubo J, Arthur W. Patterns of correlated character evolution in flightless birds: a phylogenetic approach. Evol Ecol. 2000;14: 693–702.

10. Linnaeus C. Systema naturae per regna tria naturae: secundum classes, ordines, genera, species, cum characteribus, differentiis, synonymis, locis. Stockholm: Impensis Direct; 1758.

11. Hume JP. The history of the Dodo Raphus cucullatus and the penguin of Mauritius. Hist Biol. 2006;18: 65–89.

12. Livezey BC. An ecomorphological review of the dodo (Raphus cucullatus) and solitaire (Pezophaps solitaria), flightless Columbiformes of the Mascarene Islands. J Zool. 1993;230: 247–292.

13. Kitchener AC. The external appearance of the dodo, Raphus cucullatus. Arch Nat Hist. 1993;20: 279–301.

14. Angst D, Buffetaut E, Abourachid A. The end of the fat dodo? A new mass estimate for Raphus cucullatus. Naturwissenschaften. 2011;98: 233–236.

15. Louchart A, Mourer-Chauviré C. The dodo was not so slim : leg dimensions and scaling to body mass. Naturwissenschaften. 2011;98: 357–358. doi:10.1007/s00114-011-0771-6

16. Angst D, Buffetaut E, Abourachid A. In defence of the slim dodo : a reply to Louchart and Mourer-Chauviré. Naturwissenschaften. 2011;98: 359–360. doi:10.1007/s00114-011-0772-5

17. Seebacher F. A new method to calculate allometric length-mass relationships of dinosaurs. J Vertebr Paleontol. 2001;21: 51–60.

18. Hutchinson JR, Ng-Thow-Hing V, Anderson FC. A 3D interactive method for estimating body segmental parameters in animals: Application to the turning and running performance of Tyrannosaurus rex. J Theor Biol. 2007;246: 660–680.

19. Gunga HC, Suthau T, Bellmann A, Stoinski S, Friedrich A, Trippel T, Kirsch K., Hellwich O. A new body mass estimation of Brachiosaurus brancai Janensch, 1914 mounted and exhibited at the Museum of Natural History (Berlin, Germany). Foss Rec. 2008;11: 33–38. doi:10.1002/mmng.200700011

20. Bates KT, Manning PL, Hodgetts D, Sellers WI. Estimating mass properties of dinosaurs using laser imaging and 3D computer modelling. PLoS One. 2009;4: e4532.

21. Allen V, Paxton H, Hutchinson JR. Variation in Center of Mass Estimates for Extant Sauropsids and its Importance for Reconstructing Inertial Properties of Extinct Archosaurs. Anat Rec. 2009;292: 1442–1461.

22. Sellers WI, Hepworth-Bell J, Falkingham PL, Bates KT, Brassey CA, Egerton VM, Manning PL. Minimum convex hull mass estimations of complete mounted skeletons. Biol Lett. 2012;8: 842–845.

23. Brassey CA, Sellers WI. Scaling of convex hull volume to body mass in modern primates, non-primate mammals and birds. PLoS One. 2014;9: e91691. doi:10.1371/journal.pone.0091691

24. Swainson W. On the Characters and Natural Affinities of Serveral New Birds from Australasia: Including Some Observations on the Columbidæ. Zool J. 1825;1: 463–484.

25. Fraser L. A description of a new species of Crowned Pigeon from New Guinea. Proc Zool Soc London. 1844;12: 136.

26. Shapiro B, Sibthorpe D, Rambaut A, Austin J, Wragg GM, Bininda-Emonds ORP, Lee PLM, Cooper A. Flight of the dodo. Science. 2002;295: 1683. doi:10.1126/science.295.5560.1683

27. CIBC. Seg3D: Volumetric Image Segmentation and Visualization. Scientific Computing and Imaging Institute (SCI). 2014.

28. Barber CB, Dobkin DP, Huhdanpaa HT. The Quickhull algorithm for convex hulls. ACM Trans Math Softw. 1996;22: 469–483.

29. Smith RJ. Use and misuse of the reduced major axis for line-fitting. Am J Phys Anthropol. 2009;140: 476–486.

30. Lavin SR, Karasov WH, Ives AR, Middleton KM, Garland Jr T. Morphometrics of the Avian Small Intestine Compared with That of Nonflying Mammals: A Phylogenetic Approach. Physiol Biochem Zool. 2008;81: 526–550.

31. Paradis E, Claude J, Strimmer K. APE: analyses of phylogenetics and evolution in R. Bioinformatics. 2004;20: 289–290.

32. Jetz W, Thomas GH, Joy JB, Hartmann K, Mooers AO. The global diversity of birds in space and tim. Nature. 2012;491: 444–448. doi:10.1038/nature11631

33. Hackett SJ, Kimball RT, Reddy S, Bowie RCK, Braun EL, Braun MJ, Chojnowski JL, Cox WA, Han KL, Harshman J. et al. A phylogenomic study of birds reveals their evolutionary history. Science (80-). AAAS; 2008;320: 1763.

34. Falkingham PL. Acquisition of high resolution three-dimensional models using free, open-source, photogrammetric software. Palaeontol Electron. 2012;15: 1T.

35. Mallison H, Wings O. Photogrammetry in Paleontology – A Practical Guide. J Paleontol Tech. 2014;12: 1–31.

36. Wu C. VisualSFM: A visual structure from motion system. [Internet]. 2011.

37. Brassey C, Gardiner J. An advanced shape-fitting algorithm applied to the vertebrate skeleton: improving volumetric mass estimates. R Soc Open Sci. *In press.*

505 38. Dunning J. CRC handbook of avian body masses. Boca Raton: CRC Press; 1992.

506 39. Ibrahim T, Bashrat O. Carcass characteristics of pigeons reared in Bauchi
507 Metropolis, north eastern Nigeria. Anim Prod Res Adv. 2009;5.

508 40. Omojola AB, Isa MA, Jibir M, S ABTG, Kassim OR, Omotoso AB, Adeyemo, OA,
509 Akinleye, SB. Carcass Characteristics and Meat Attributes of Pigeon (Columbia
510 livia) as Influenced by Strain and Sex. J Anim Sci Adv. 2012;2: 475–480.

511 41. Roth VL. Insular dwarf elephants: a case study in body mass estimation and
512 ecological inferenc. In: Damuth J, MacFadden B, editors. Body size in mammalian
513 paleobiology: Estimates and biological implications. Cambridge: Cambridge
514 University Press; 1990. pp. 151–180.

515 42. Herbert T. A relation of some yeares' travaile, begunne Anno 1626, into Afrique
516 and the greater Asia, especially the territories of the Persian Monarchie, and
517 some parts of the Oriental Indies and Isles adiacent. London: W Stansby & J
518 Bloome; 1634.

519 43. Kirkwood JK, Duignan PJ, Kember NF, Bennett PM, Price DJ. The growth rate of
520 the tarsometatarsus bone in birds. J Zool. 1989;217: 403–416.
521 doi:10.1111/j.1469-7998.1989.tb02498.x

522 44. Campbell KE, Marcus L. The relationship of hindlimb bone dimensions to body
523 weight in birds. In: Campbell KE, editor. Papers in avian paleontology honouring
524 Pierce Brodkorb Science Series 39. Los Angeles: Natural History Museum of Los
525 Angeles; 1992. pp. 395–411.

526 45. Brassey CA, Kitchener AC, Withers PJ, Manning PL, Sellers WI. The Role of
527 Cross-Sectional Geometry, Curvature, and Limb Posture in Maintaining Equal
528 Safety Factors: A Computed Tomography Study. Anat Rec. 2013;296: 395–413.

529 46. Hamershock DM, Seamans TW, Bernhard GE. Determination of body density for
530 twelve bird species. Flight Dynamics Directorate, Wright Laboratory. Flight
531 Dynamics Directorate, Wright Laboratory; 1993.

532 47. Henderson D. Burly Gaits: Centers of mass, stability, and the trackways of
533 sauropod dinosaurs. J Vertebr Paleontol. The Society of Vertebrate Paleontology;
534 2006;26: 907–921.

535 48. Randall A, Pepe A, Yamartino K, Kimelblatt A, Claeesens L. How fat was the
536 Dodo? The first mass estimate from digital body reconstruction based on a
537 complete skeleton of Raphus cucullatus. Society of Vertebrate Paleontology
538 Annual Meeting 2014, Berlin Poster Abstract. 2014.

539 49. Benson RBJ, Campione NE, Carrano MT, Mannion PD, Sullivan C, Upchurch P,
540 Evans DC. Rates of dinosaur body mass evolution indicate 170 million years of
541 sustained ecological innovation on the avian stem lineage. PLoS Biol. 2014;12:
542 e1001853. doi:10.1371/journal.pbio.1001853

543 50. Rosset A, Spadola L, Ratib O. OsiriX: an open-source software for navigating in
544 multidimensional DICOM images. J Digit Imaging. 2004;17: 205–216.

Figure 1. Example of the convex hulling process applied to the CT scanned carcass of a Victoria crowned pigeon (*Goura victoria*) from which the skeleton has been segmented. A and C, skeleton in dorsal and lateral view respectively and; B and D, corresponding convex hulls fitted to the functional units of the skeleton. Note convex hulls fitted to the feet in 1D are strongly influenced by the positioning of the toes (see in text for discussion).

Figure 2. OLS regression results. Body mass (g) against convex hull volume (mm^3). For slope equations see Table 2. Filled circles and solid line, eviscerated carcasses; crosses and dashed line, intact carcasses; dot-dash line, combined sample.

Figure 3. A, Photogrammetry model of the Tring dodo skeleton (S/1988.50.1); B, volumetric convex hulls fitted around the skeleton.

Figure 4. The distribution of segment CH_{vol} as a proportion of total CH_{vol} within the convex hulled skeletons of extant pigeons and articulated dodo skeletons. Mean values are illustrated for extant pigeons. Error bars represent 95% confidence intervals of the mean. The underdevelopment of the pectoral girdle (humerus, radius and ulna and carpometacarpals) in dodo relative to extant pigeons is particularly striking.

Figure 5. Volumetric renderings of a rock dove (*Columba livia, A-B*) and collared dove (*Streptopelia decaocto*, *C-D)* generated from CT scans. A and C illustrate the outer soft tissue contours of the carcass, while B and D illustrate the position of the gizzard and associated gizzard contents. There is considerable variation in the quantity and size of

565 gizzard stones between intact pigeon specimens within the dataset. Renderings were
566 generated in OsiriX [50]

Table 1(on next page)

Specimen list of modern pigeons

Table 1. Specimen list of modern pigeons sourced from National Museums Scotland, Edinburgh. CH_{vol}, minimum convex hull volume of the skeleton; CH_{vol} – feet, minimum convex hull volume minus the volume of the feet. * indicates specimens were sourced from the University of Manchester. All other specimens were loaned from National Museums Scotland, Edinburgh.

1

Species name	Common name	Body mass (g)	Preparation	CH_{vol} (mm^3)	CH_{vol} – feet (mm^3)
Goura victoria	Victoria crowned pigeon	1951	Eviscerated	1487180	1436777
*Streptopelia decaocto**	Collared dove	201	Intact	203875	196791
Columba livia	Rock dove	290	Intact	115945	113074
*Columba palumbus**	Wood pigeon	305	Intact	337993	328279
Ducula bicolor	Pied imperial pigeon	450	Eviscerated	337377	329220
Petrophassa rufipennis	Chestnut-quilled rock pigeon	314	Eviscerated	303511	286104
Otidiphaps nobilis	Pheasant pigeon	401	Eviscerated	344368	329238
Nesoenas mayeri	Pink pigeon	200	Eviscerated	197171	185981
Ducula sp.	Imperial pigeon	336	Eviscerated	314985	305344
Caloenas nicobarica	Nicobar pigeon	539	Eviscerated	383736	367753
Phaps chalcoptera	Common bronze-winged pigeon	249	Intact	213953	208942
Ducula aenea	Green imperial pigeon	483	Intact	348268	336968
Columba guinea	Speckled pigeon	158	Intact	105156	102041
Zenaida graysoni	Socorro dove	176	Eviscerated	105776	102441

Gallicolumba sp.	Bleeding heart dove	215	Eviscerated	163764	152136
Phapitreron leucotis	White-eared brown dove	107	Eviscerated	69424	67088
Ptilinopus sp.	Fruit dove	71	Eviscerated	47816	46635
Ptilinopus superbus	Superb fruit dove	137	Eviscerated	77882	74691
Treron vernans	Pink-necked green pigeon	167	Eviscerated	104991	101984
Ocyphaps lophotes	Crested pigeon	107	Intact	67451	64011

Table 1. Specimen list of modern pigeons sourced from National Museums Scotland, Edinburgh. CH_{vol}, minimum convex hull volume of the skeleton; CH_{vol} – feet, minimum convex hull volume minus the volume of the feet. * indicates specimens were sourced from the University of Manchester. All other specimens were loaned from National Museums Scotland, Edinburgh.

Table 2 (on next page)

Details of mass prediction equations

Ordinary least squares regressions of $\log_{10}$ body mass (g) against $\log_{10}$ convex hull volume (CH_{vol}, mm^3). ±95%, 95% confidence intervals of the intercept and slope; MSE, mean square error of the regression; AIC, Akaike Information Criterion calculated for Ordinary Least Squares (OLS) and Phylogenetically Generalised Least Squares (PGLS). Ground-dwelling refers to the predictive equation based upon ratites and fowl derived from [23] .

Model	*a*	*a* (±95%)	*b*	*b* (±95%)	r^2	*p*	AIC_{OLS}	AIC_{PGLS}
Eviscerated	-2.31	-2.90 - -1.72	0.89	0.78-1.00	0.97	<0.001	-28.42	-20.97
- minus feet	-2.31	-2.87 - -1.74	0.90	0.79-1.00	0.97	<0.001	-29.38	-22.22
Intact	-1.08	-3.69 - -1.53	0.66	0.16-1.16	0.70	0.019	-5.29	-10.15
- minus feet	-1.06	-3.62 - -1.50	0.66	0.17-1.15	0.70	0.018	-5.41	-10.41
Combined	-2.08	-2.75 - -1.42	0.85	0.72-0.98	0.92	<0.001	-34.42	-26.64
- minus feet	-2.08	-2.73 - -1.42	0.85	0.73-0.98	0.92	<0.001	-34.94	-27.39
Ground-dwelling	-1.65	-2.52 - -0.77	0.82	0.69-0.95	0.97	<0.001		

Table 2. Ordinary least squares regressions of $\log_{10}$ body mass (g) against $\log_{10}$ convex hull volume (CH_{vol}, mm^3). ±95%, 95% confidence intervals of the intercept and slope; MSE, mean square error of the regression; AIC, Akaike Information Criterion calculated for Ordinary Least Squares (OLS) and Phylogenetically Generalised Least Squares (PGLS). Ground-dwelling refers to the predictive equation based upon ratites and fowl derived from [23].

Table 3 (on next page)

Predicted body mass of the dodo

M_b estimated using 'eviscerated' equation minus feet (Table 2) and applying correction factor e(MSE/2) to account for back-transformation of a log-linear model into a power function, where MSE is the mean square error reported in Table 2. 95%PI, 95% prediction intervals. Ground-dwelling refers to the predictive equation based upon ratites and fowl derived from [23] . *Calculated on the basis of dodo CH_{vol} including feet, as per the modern ground-dwelling birds.

1

Model	Accession number	CH_{vol} (mm^3)	CH_{vol} – feet (mm^3)	Eviscerated M_b (g)	95% PI (g)	Ground-dwelling M_b (g) *	95% PI (g)
NHMUK Tring dodo	S/1988.50.1	8942820	8445134	7980	4653- 13685	10869	5737-20593
NHMUK Kensington dodo	NHM A.9040	9730367	9283795	8687	5027-15011	11646	6141-22084
Edinburgh dodo	NMS.Z.1993.13	12147000	11787000	10760	6106-18961	13960	7338-26560

2 Table 3. M_b estimated using 'eviscerated' equation minus feet (Table 2) and applying correction factor e(MSE/2) to
3 account for back-transformation of a log-linear model into a power function, where MSE is the mean square error reported
4 in Table 2. 95%PI, 95% prediction intervals. Ground-dwelling refers to the predictive equation based upon ratites and fowl
5 derived from [23]. *Calculated on the basis of dodo CH_{vol} including feet, as per the modern ground-dwelling birds.

6

1

Convex hulling process

Example of the convex hulling process applied to the CT scanned carcass of a Victoria crowned pigeon (*Goura victoria*) from which the skeleton has been segmented. A and C, skeleton in dorsal and lateral view respectively and; B and D, corresponding convex hulls fitted to the functional units of the skeleton. Note convex hulls fitted to the feet in 1D are strongly influenced by the positioning of the toes (see in text for discussion).

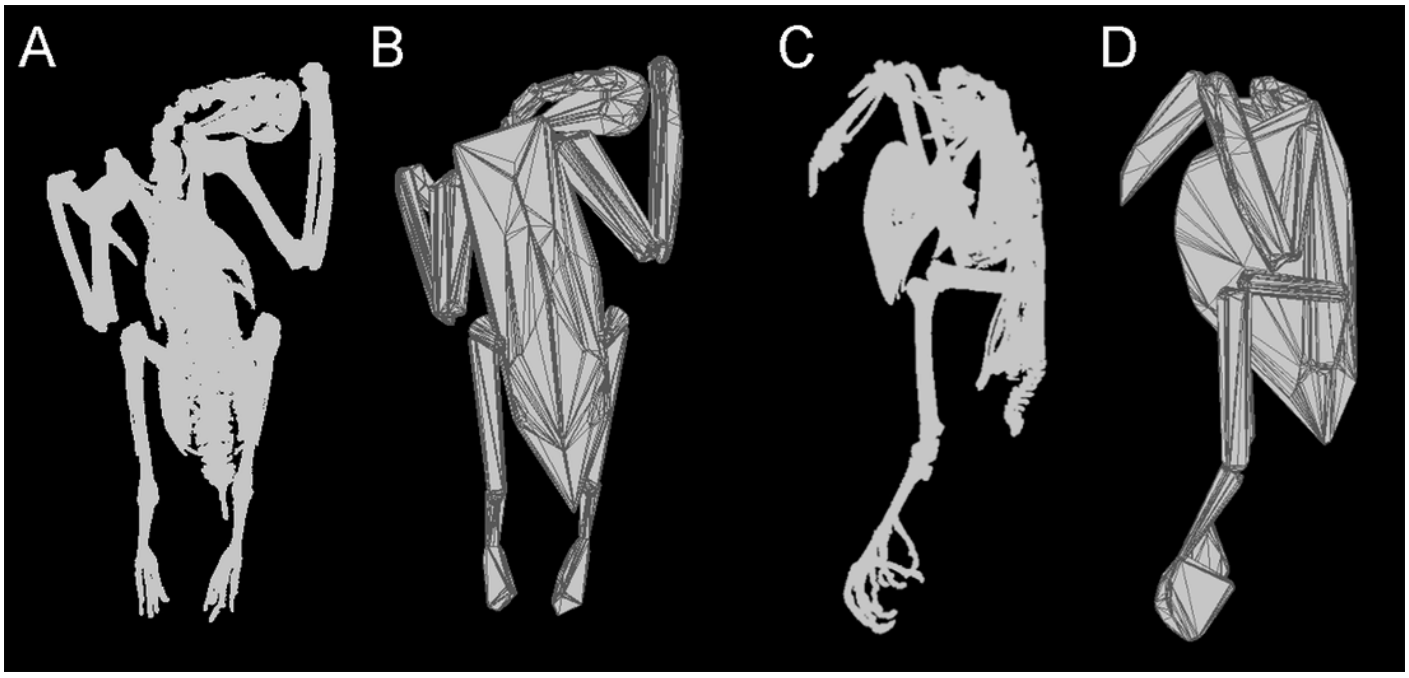

2

Convex hull predictive model

OLS regression results. Body mass (g) against convex hull volume (mm^3). For slope equations see Table 2. Filled circles and solid line, eviscerated carcasses; crosses and dashed line, intact carcasses; dot-dash line, combined sample.

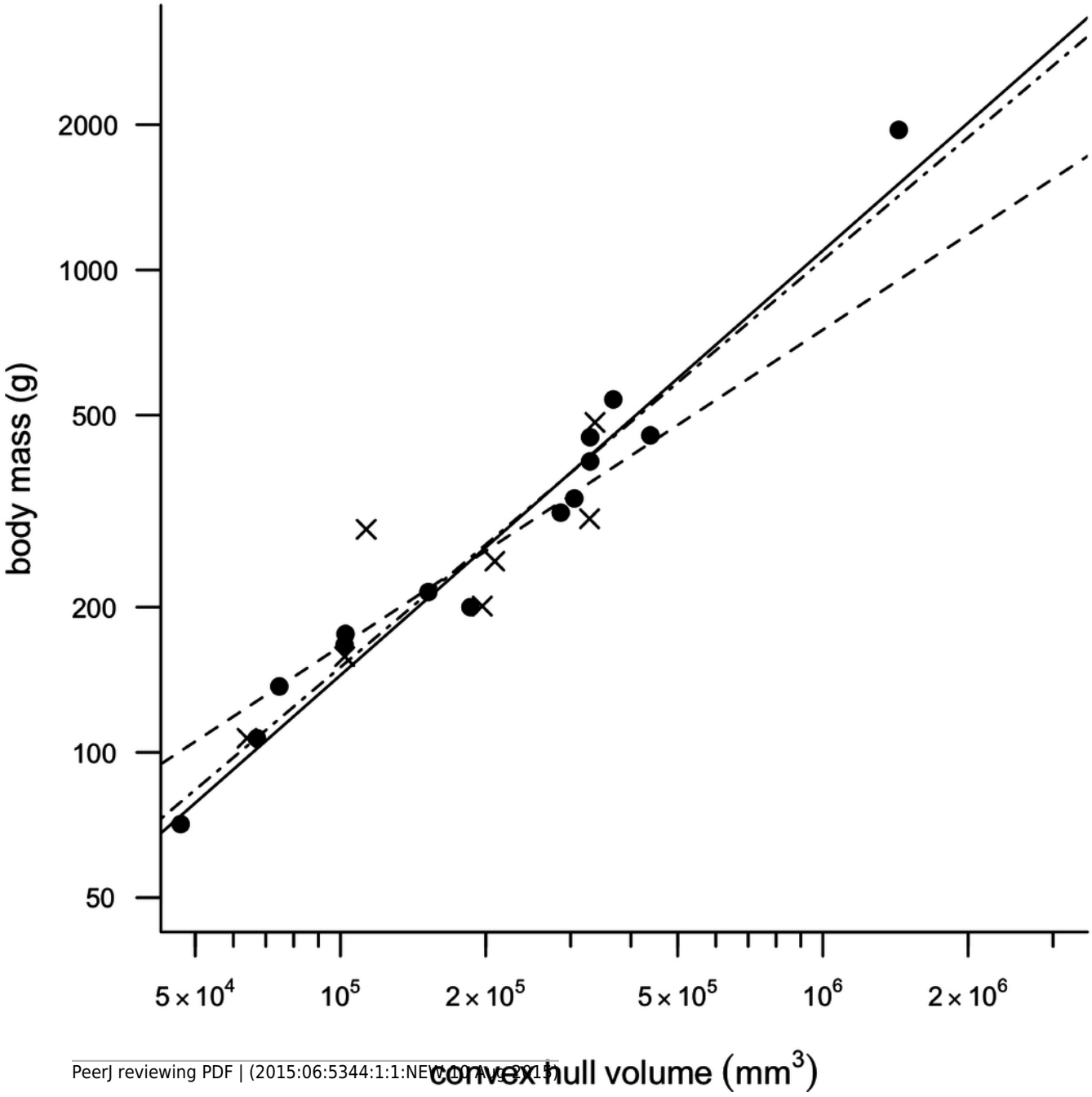

3

Convex hull model of Tring dodo

A, Photogrammetry model of the Tring dodo skeleton (S/1988.50.1); B, volumetric convex hulls fitted around the skeleton.

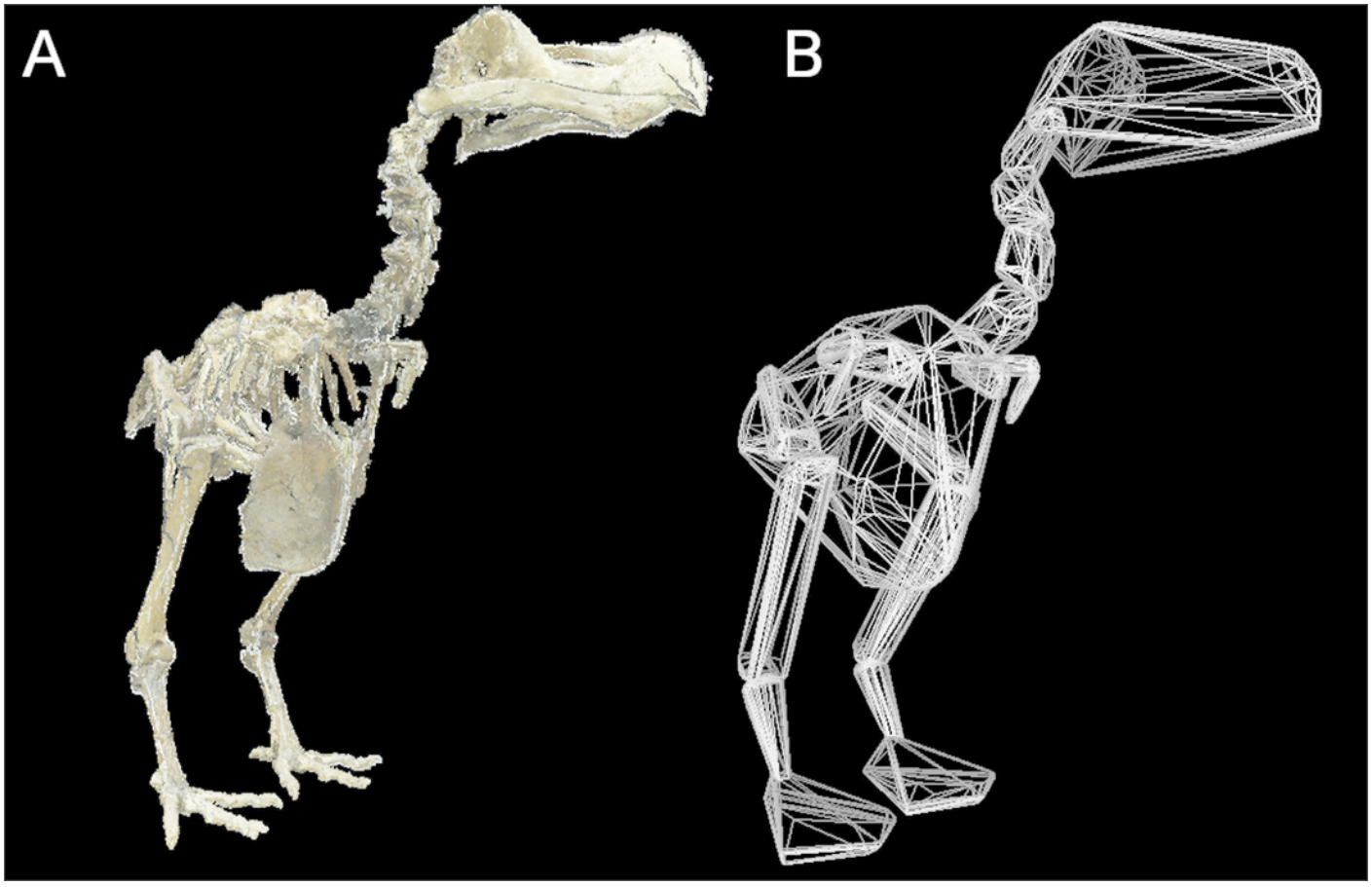

4

Distribution of convex hull volume around the pigeon skeleton

The distribution of segment CH_{vol} as a proportion of total CH_{vol} within the convex hulled skeletons of extant pigeons and articulated dodo skeletons. Mean values are illustrated for extant pigeons. Error bars represent 95% confidence intervals of the mean. The underdevelopment of the pectoral girdle (humerus, radius and ulna and carpometacarpals) in dodo relative to extant pigeons is particularly striking.

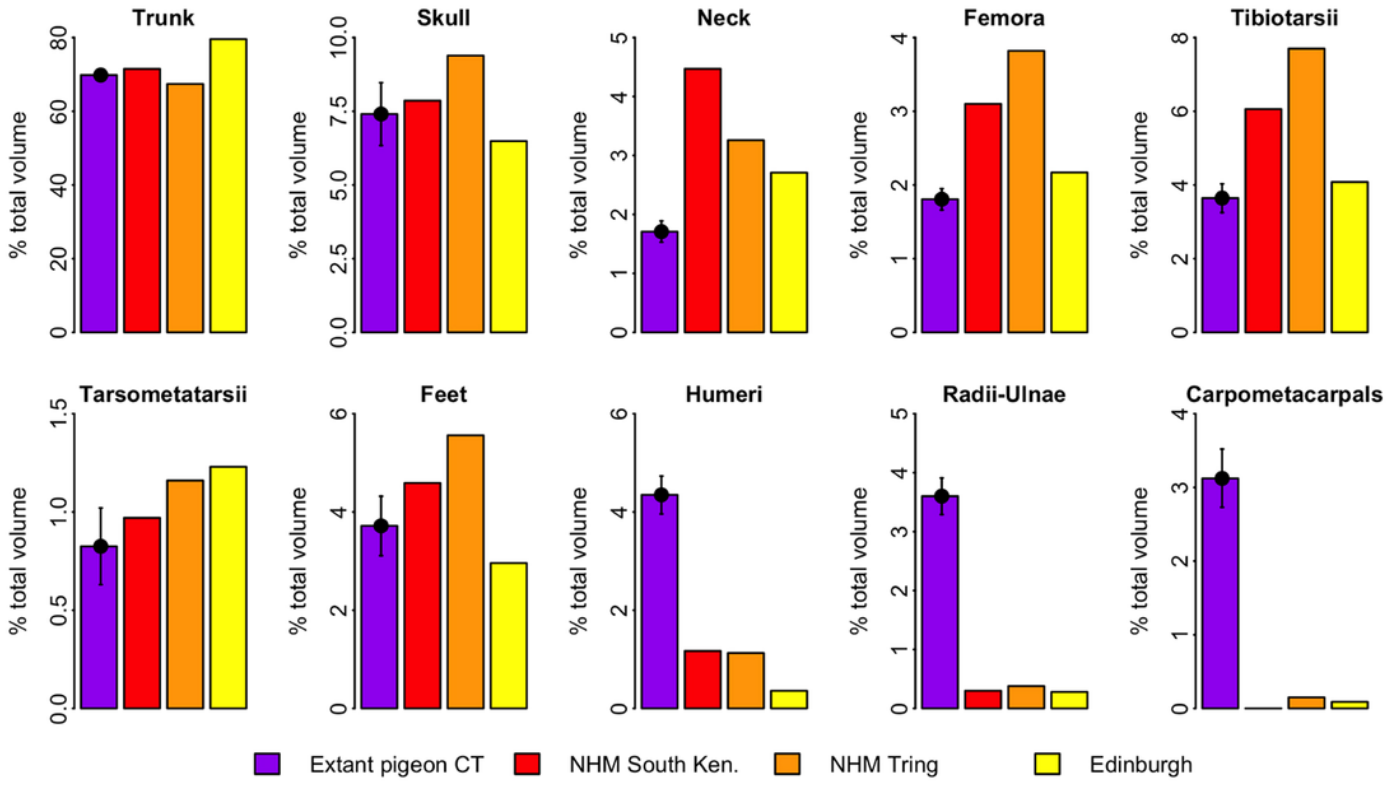

5

Volume renderings of modern pigeon CT data

Volumetric renderings of a rock dove (*Columba livia, A-B*) and collared dove (*Streptopelia decaocto*, *C-D)* generated from CT scans. A and C illustrate the outer soft tissue contours of the carcass, while B and D illustrate the position of the gizzard and associated gizzard contents. There is considerable variation in the quantity and size of gizzard stones between intact pigeon specimens within the dataset. Renderings were generated in OsiriX [50]